Exhibit 530

Self-assembling peptide semiconductors

https://pubmed.ncbi.nlm.nih.gov/29146781/

Science. Author manuscript; available in PMC 2017 Dec 2.
Published in final edited form as:
Science. 2017 Nov 17; 358(6365): eaam9756.
doi: 10.1126/science.aam9756

PMCID: PMC5712217
EMSID: EMS74989
PMID: 29146781

Self-assembling peptide semiconductors

Kai Tao,[1] Pandeeswar Makam,[1] Ruth Aizen,[1] and Ehud Gazit[1,2,*]

Abstract

Semiconductors are central to the modern electronics and optics industries. Conventional semiconductive materials bear inherent limitations, especially in emerging fields such as interfacing with biological systems and bottom-up fabrication. A promising candidate for bioinspired and durable nanoscale semiconductors is the family of self-assembled nanostructures comprising short peptides. The highly ordered and directional intermolecular π-π interactions and hydrogen-bonding network allow the formation of quantum confined structures within the peptide self-assemblies, thus decreasing the band gaps of the superstructures into semiconductor regions. As a result of the diverse architectures and ease of modification of peptide self-assemblies, their semiconductivity can be readily tuned, doped, and functionalized. Therefore, this family of electroactive supramolecular materials may bridge the gap between the inorganic semiconductor world and biological systems.

Although widely used in many fields, conventional inorganic semiconductors have several shortcomings, such as the requirement for relatively complex crystal growth and the use of toxic metals (1, 2). Organic polymeric semiconductors overcome some of these disadvantages, but several issues—including weak oxidation stability or sustainability, a narrow color spectrum, the demand for heavy metal doping, and, in some cases, complicated synthesis procedures—still impede their operational aspects and commercial manufacture (3). Supramolecular organic organizations, such as the self-assembly of phthalocyanines (4–6), have been recognized as potential alternatives. However, their non-biological nature presents obstacles for advanced technological applications such as interfacing of electronic devices with living systems, electroactive tissue engineering, and the development of imaging agents (7).

Bioinspired supramolecular chemistry can allow for a better interface between the semiconductive and biological worlds. In particular, simple peptide building blocks with the intrinsic ability to self-assemble into ordered nanostructures emerge as promising candidates (Fig. 1) (8, 9). The ample constituents, various morphologies, precise molecular structures, and biomolecular recognition endow the peptide self-assemblies with diversified physicochemical features. Integration with external semiconductive subunits, such as perylene imide moieties (10–14), can yield self-assembled products with tunable morphologies and en-

hanced semiconductivity. In addition, with the intrinsic advantages of ease of preparation and flexibility of structure-function modulation, these bioinspired materials can be used in biotechnological and medical fields.

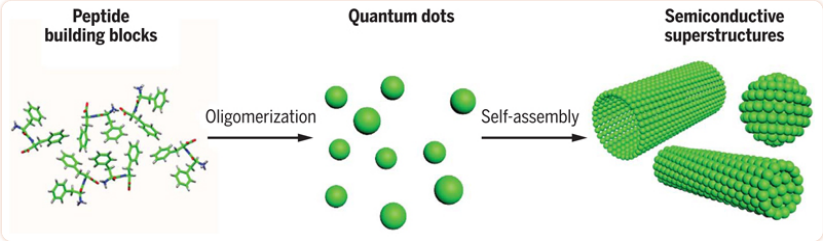

Fig. 1

Peptide self-assembling architectures show intrinsic semiconductive properties.

Peptide building blocks oligomerize to quantum dots, which then self-assemble into supramolecular structures with diverse morphologies to serve as the bioinspired organic semiconductors.

Recent studies have revealed that several natural protein aggregates possess intrinsic semiconductive optical properties (15). Kaminski *et al*. demonstrated that when excited at 405 nm, the assemblies of misfolded proteins associated with neurodegenerative disorders can exhibit intrinsic fluorescent emission (16, 17). This label-free autofluorescence allows quantitative assessment of the kinetics of amyloid fibrillar formations, eliminating the need for extrinsic labeling, which might result in steric hindrance and other perturbations during aggregation (16).

Self-assembled structures made of very short peptides, including fragments of such amyloidogenic proteins, may also have intriguing semiconductive properties because their band gaps are comparable to those of conventional materials (18). Furthermore, their bioderived nature and rigid self-assembly (19, 20) can minimize the potential cytotoxicity of the building blocks (21), demonstrating the biocompatibility of the supramolecular structures. Enantiomers determine the enzymatic sensitivity (L-type) or resistance (D-type) of self-assemblies (22), thus underlying their controllable biosustainability. Also, the weak reducibility of the amino acids implies the strong oxidation stability of the supramolecular structures (23). By virtue of their simple and low-cost synthesis, as well as their ease of modulation relative to their larger counterparts, these self-assembled peptide semiconductors may serve as candidates for advanced interdisciplinary functional nanostructures (24, 25).

Short peptides can form diverse nanostructures

Semiconductive properties are highly dependent on material morphology (26). Consequently, the numerous nanostructures formed by the self-assembly of short peptide building blocks can give rise to versatile semiconductive features (27).

The most studied short peptides that self-associate into semiconductive nanomaterials are aromatic short peptides (27). Diphenylalanine (FF), a minimal aromatic dipeptide derived from the β-amyloid (Aβ) self-assembling polypeptide (22), forms abundant self-assembling semiconductive architectures (27–29). Different methodologies have been used to investigate and facilitate the self-assembly of FF and its derivatives. One approach is the use of different solvents, in which FF was shown to self-assemble into distinct nanostructures (Fig. 2A) (30–32).

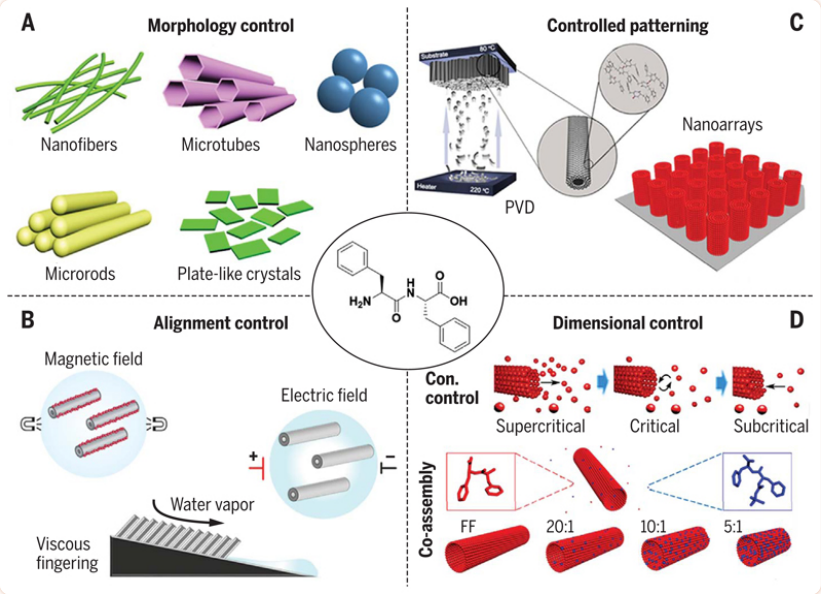

Fig. 2

Modulation of FF self-assembly via diverse methodologies.

(A) Morphology control using different solvents. [Adapted from (30–32)] **(B)** Alignment control over FF nanotube directions via external fields or different crystallization patterns. [Adapted from (33–36)] **(C)** Controlled patterning of FF self-assemblies by the PVD assembly technique and the deposited vertical nanoarrays. The circular insets show the molecular structures of the nanoarrays. [Adapted from (37)] **(D)** Dimensional control of FF nanotubes by controlling the concentrations and by the coassembly method. [Adapted from (42, 44)]

FF self-assemblies can be further directionally aligned. For example, FF nanotubes can be orderly arrayed in an external field as a result of induced polarization within the nanostructures (Fig. 2B) (33, 34). In addition, different morphologies, including vertically aligned arrays, centrosymmetric pattern assemblies, spoke-like patterns, and ordered adjoining microrods, can be formed from a hexafluoroisopropanol solution of FF by controlling solute convection (Fig. 2B) (33, 35, 36). Notably, all of these superarchitectures share the same crystallographic lattice structures, implying a simple strategy to prepare complicated nanostructures by controlling the dewetting process of the FF solution (35). The nanoarrays can also be manufactured by physical vapor deposition (PVD) of FF powders (Fig. 2C) (37), allowing for further modulation of dimensional parameters such as morphology (nanotubes or nanowires), arraying density, and aspect ratio (38–40).

The dimensions of FF nanotubes are more directly affected by the concentration (41). Using microfluidics to fine-tune differential local environments, the concentration-dependent growth and shrinkage of FF nanotubes can be detected in real time (Fig. 2D, top) (42).

A coassembly strategy can be used to generate additional morphologies (25). Coassembly of FF and FFF (*tri*-phenylalanine) can form diverse nanostructures in a ratio-dependent manner, because FFF generates a negative curvature where its bulky hydrophobic side chains are more closely packed and avoid exposure to water molecules (43). Therefore, increasing the percentage of FFF can modulate the coassemblies from hollow to solid morphologies. As a result, toroid nanostructures, a rarely reported supramolecular structure, can be formed when the FFF ratio is 0.167 to 0.33 (43). In addition, coassembly of FF and *tert*-butyloxycarbonyl-FF (Boc-FF) can modulate the FF nanotube elongation, with the length decreasing as the Boc-FF molar ratio increases, thus providing a controllable nanotube length distribution (Fig. 2D, bottom) (44).

Chemical conjugation can provide another effective approach for the modulation of FF self-assembly (25). Specifically, the terminal groups can be modified with diverse functional moieties (45–51), resulting in a propensity of FF to self-assemble into various nanostructures (29). For example, Boc-FF initially forms nanospheres, then nanofibers, and finally evolves to well-crystallized nanotubes (47). In addition to the backbone termini, the side chains of FF can be modified, with a remarkable impact on the self-assembly. In particular, substitution of the phenyl rings with nucleobases generated a new family of bioinspired building blocks—peptide nucleic acids (PNAs) (52)—which can self-associate into well-organized entities coordinated by both Watson-Crick hydrogen bonding and aromatic stacking. For example, in guanine-cytosine (GC *di*-PNA) plate-like crystals, the hydrogen bond length between symmetry-related bases is ~2.9 Å, consistent with typical Watson-Crick base pairs, and the base distance is ~3.5 Å, the same as in DNA double-helix structures (53).

Mechanisms underlying semiconductivity

An understanding of the self-assembly mechanisms and associated microscopic molecular structures of the short peptide nanostructures is required in order to elucidate the basis of their semiconductive properties. Several studies have revealed that the dimers, which function as quantum dots (QDs), serve as the elementary building blocks of FF self-assembly (54). The aggregation process can undergo a series of supramolecular phases and is driven by T-shaped aromatic stacking in combination with interpeptide head-to-tail and peptide-water hydrogen-bonding interactions (55). The self-assembly results in the formation of porous nanotubular crystals (56), with pores consisting of an amide backbone “tube” surrounded by six “zipper-like” aromatic interlocks each composed of two diphenyls (Fig. 3A) (57). This interlocking can induce the π-electrons to delocalize during self-assembly. The assembly-disassembly process (i.e., the phase transformation between QDs and nanotubes) can be reversed by controlling the solution conditions, such as the peptide concentration or the solvent (54, 55). The “zipper-like” aromatic interlock structures are the molecular basis of the quantum confined structures, thus underlying the semiconductivity of FF assemblies.

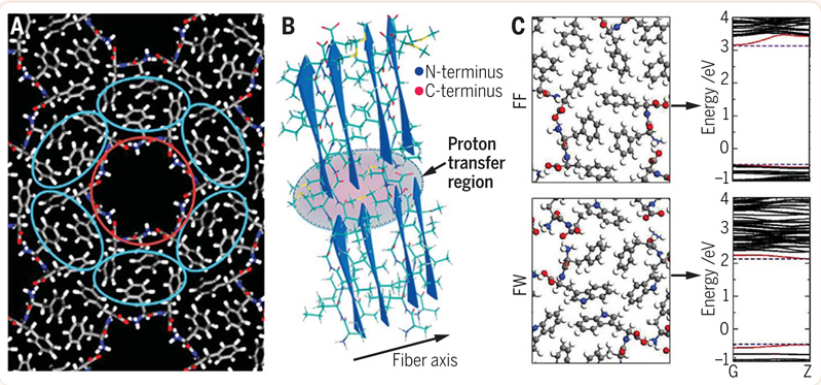

Fig. 3

Molecular mechanisms underlying short peptide self-assembling semiconductors.

(**A**) Model showing the construction of FF nanotubular crystals. The quantum confined structures comprise a backbone-based "tube" (red circle) surrounded by six "zipper" units, each composed of two diphenyls (cyan circle). [Adapted from (57)] (**B**) Schematic depiction of the cross section of two adjacent β sheets in peptide self-assemblies. The shaded ellipsoid illustrates the quantum confined region where proton transfers occur. [Adapted from (59)] (**C**) Quantum confined regions for FF (top) and FW (bottom) nanotubular crystals, showing more compact aromatic interlocking structures for FW. The altered aromatic interactions induce a remarkable difference between the conduction band minima and valence band maxima along the tube axis, indicating a smaller band gap for FW self-assembly relative to FF. [Adapted from (61)]

The self-assembly of peptides containing non-aromatic residues cannot be derived from aromatic interlocking interactions (15). The physicochemical properties of this kind of nanostructure result from the electronic levels in the peptide bonds that become available through backbone-backbone hydrogen bonds in the secondary structures (58). The intrinsic fluorescence of amyloid nanofibers in the visible spectrum arises from the transfer of protons from hydrogen bonds among b sheets (59). As a result of this transfer, the proton can exist at either the N or C terminus of strands between adjacent β sheets, thus creating a double-well ground-state potential that can avoid the potential energy intersection with the excitation state and promote the red shift of the exciton transition (59). These localized proton-transfer regions, combined with the N and C termini of strands between adjacent b sheets, constitute the quantum confined structures underlying the molecular origin of semiconductivity (Fig. 3B).

Thus, the prerequisite for short peptide self-assembling semiconductors is that the driving forces, including aromatic interlocks and hydrogen bonding, decrease the band gaps down to the semiconductive region. Consequently, the semiconductivity of the superstructures can be tuned by controlling the driving forces. For instance, density functional theory calculations demonstrated that when replacing FF with FW (phenylalanine-tryptophan), reinforced aromatic interactions and more compact molecular interstitial regions enhance the conductivity by a factor of 5 relative to FF assemblies (60), with a decline in the band gap from 3.25 eV to 2.25 eV (Fig. 3C) (61). Moreover, increasing the water molecule hydrogen bonding in the channel cores by increasing the relative humidity can split and redshift the photoluminescence peak of FF nanotubes, leading to increased band gaps (62).

Semiconductive properties and applications of peptide self-assemblies *Absorption spectra of quantum confined structures*

The nano-sized quantum confined structures of short peptide self-assemblies result in structure-dependent optical characteristics attributable to the strong Coulomb interaction between highly confined electrons and holes, which can lead to the formation of an exciton with specific absorption and luminescence (25, 63). For example, spike-like absorbance spectra are observed for FF nanotubes (54) and Boc-FF nanospheres (48), indicating that zero-dimensional QDs exist in the assemblies. Calculations have demonstrated that the radii of the QDs formed by FF and Boc-FF molecules are approximately 1.65 and 1.3 nm, respectively, implying that the QDs are composed of two monomers (54). In contrast, the absorption spectra of Fmoc-FF nanofibrillar hydrogels exhibit a pronounced step-like absorption pattern, accompanied by a peak at the long-wavelength edge derived from the strengthened Coulomb interaction of excitons—a characteristic of two-dimensional quantum well confinement structures (64).

Photoluminescent properties

Short peptide self-assembling semiconductors also have intriguing photoluminescent properties. For example, when excited at 255 nm, FF nanotubes show fluorescent emission, with one band at the near-ultraviolet (centered at 290 nm) and the other in the visible region (350 to 500 nm) (65). The FF tubular nanoarrays that form quantum well confinement structures can emit blue fluorescence when excited at 340 to 380 nm (Fig. 4A), an advantageous feature for backlight display applications such as light-emitting diodes (66). Notably, the photoluminescence is easily controlled, showing enhanced intensity with increasing thickness (67) or decreasing temperature (65). Another interesting example is GC *di*-PNA crystals, where the introduction of further aromatic interactions and hydrogen bonding via Watson-Crick base-pairing results in broad-spectrum emission in the visible region, showing red-edge excitation shifts from 420 to 684 nm (Fig. 4B) (53).

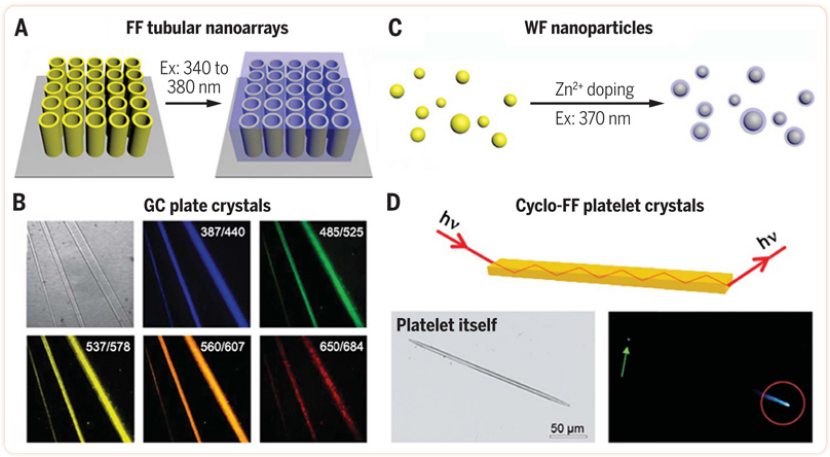

Fig. 4

Optical properties of self-assembling short peptide semiconductors.

(**A**) Schematic depiction of the photoluminescence from the patterned surface of FF tubular nanoarrays on silicon substrate upon excitation at 340 to 380 nm. [Adapted from (66)] (**B**) Bright-field and corresponding fluorescent images of GC *di*-PNA crystals. Each fluorescent image was taken with different excitation/emission filters, as noted. Pseudocolors represent the corresponding emission color. Magnification, ×100. [Adapted from (53)] (**C**) Schematic representation of the self-assembly of the tryptophan-phenylalanine dipeptide to photoluminescent spherical NPs via Zn^{2+} coordination. [Adapted from (70)] (**D**) Cartoon model (top), bright-field image (lower left), and confocal microscopy image (lower right) of the optical waveguiding of cyclo-FF crystallized platelets. The red circle marks the excitation area; the green arrow denotes the outcoupling of emission at the other end. [Adapted from (71)]

Doping has been shown to be a highly effective approach for enhancing the properties of semiconductors (68, 69). When complexed with zinc ion, tryptophan-phenylalanine self-assembling nanoparticles (NPs) emit blue fluorescence at 423 nm after excitation at 370 nm (Fig. 4C) (70). The quantum yield is calculated to be ~12%, versus only 9% for the native NPs. Notably, the doped NPs show better photostability than traditional organic fluorescent dyes and better biocompatibility than inorganic QDs, exhibiting a narrow photoluminescence spectrum and superior stability against pH and temperature (70). Furthermore, when functionalized with the mucin 1 (MUC1) aptamer or doxorubicin, the doped NPs can be used to target cancer cells, allowing real-time imaging and monitoring of drug release (70).

The delocalized π-electrons of aromatic systems and free proton transfer of hydrogen bonds during self-assembly indicate that peptide supramolecular semiconductors can transmit photons by continuous emission along the axis under excitation, allowing them to serve as optical wave-guides (28). For example, when focusing an excitation of 330 to 380 nm to one end of a cyclo-FF platelet crystal, a guided blue light is emitted from the other end (Fig. 4D), and the emission can be modified to other wavelengths by incorporating various dyes (71), implying a potential use of short peptide self-assemblies in applications such as light harvesting (solar cells) and energy transfer (optical cables).

Conductive properties

Another key feature of semiconductors is their increasing electrical conductivity upon temperature elevation, opposite to classical conductors (72). For example, the cyclo-FF crystallized nanowires exhibit increased electric conductivity, from ~1.5 nA to ~5.0 nA at a voltage of 10 V, as the temperature increases from 273 K to 387 K (73).

The self-assembly morphology can have a marked influence on conductance. The superstructures self-assembled by AAKLVFF, an Aβ-derived heptapeptide, can affect the conductivity, with long and straight nanofibers being the most conductive; as the assemblies become shorter or curved, the resistance increases (74). In addition, the side-chain groups, especially aromatic moieties, can also affect the conductivity, exhibiting improved conductive performance upon incorporation of non-natural 2-thienylalanine [(2-Thi)(2-Thi)VLKAA] (75). Further studies demonstrate that both protons and electrons can function as charge carriers, revealing a hybrid current transport mechanism in the nanofibers (75). This hybrid behavior leads to a bimodal exponential dependence of the conductance on the relative humidity, with a crossover point at relative humidity of ~60% (75). Below the crossover point, both electrons and protons contribute to the conduction, with the latter contribution persisting even under vacuum conditions. Above the crossover point, proton transport becomes the dominant mode, with much higher dependence on relative humidity (75). Both the conduction and the exponential dependence on relative humidity are affected by the extent of folding of the peptide network, demonstrating that the fully folded nanofibers displayed higher conductance (75).

Ferroelectric properties

The directional hydrogen-bonding and aromatic interaction networks demonstrate that the self-assembling peptide nanostructures have a specific alignment of dipoles (76), which can produce spontaneous polarization underlying their intrinsic ferroelectric properties (76, 77). For example, the FF self-assembling nanotubes have unidirectional-handed helical $–NH^{3+}\cdots^{-}OOC$ hydrogen-bonding dipoles within the noncentrosymmetric crystal (Fig. 5A, top), and hence exhibit a partial switch of polarization along the hexagonal axis under a sizable coercive field lattice (Fig. 5A, bottom) (77). Furthermore, a light-induced Stark effect can be observed, leading to a reduction in the intensity of the polarization field due to the variation in the hydrogen bonds, wherein the saturated polarization–electric field loops can be obtained at a lower coercive field (4.28 V) by combining the action of light during the hysteresis loop measurements (Fig. 5B) (77). In particular, the excellent reproducibility of the photoresponsive cycles of ferroelectricity in FF nanotubes can allow the design of optical rewritable multistate memories.

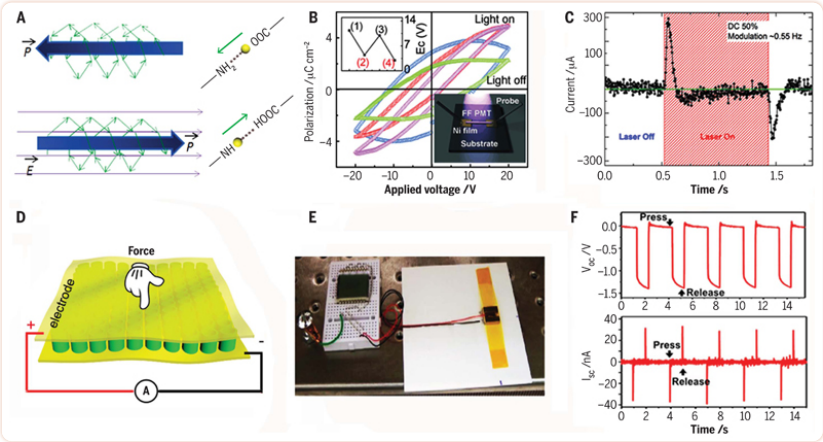

Fig. 5

Ferroelectric properties of FF self-assemblies.

(**A**) Mechanism explaining the origin of spontaneous polarization and the predictable ferroelectricity of FF nanotubes. The short green arrows represent electric dipole moments of the hydrogen bonds; long blue arrows denote net electric polarization in the nanochannel. The spontaneous polarization in a nanotube is shown on the upper side, whereas the lower side shows that displacement of protons switches the spontaneous polarization under an alternative electric field (purple arrows). [Adapted from (77)] (**B**) Four polarization-electric curves obtained from the FF tubes during off/on switching of light. The inset shows the light-induced coercive field variations with sequent light-off (1, 3) and light-on (2, 4) switching and a schematic of the device structure. [Adapted from (77)] (**C**) Representative waveform of the pyroelectric current of the FF microtubes bundle under laser irradiation. [Adapted from (79)] (**D**) Schematic of the piezoelectricity measurement of vertical FF arrays with controlled forces. [Adapted from (81)] (**E**) Photograph of the prototypical generator using vertical FF arrays as a direct power source for an LCD. [Adapted from (81)] (**F**) Open-circuit voltage (top) and short-circuit current (bottom) from the generator in (**E**). [Adapted from (81)]

The temperature-dependent change in the spontaneous polarization of the self-assemblies can produce pyroelectricity (78). A recent study using laser pulse illumination to control the temperature discovered a remarkable temperature-dependent pyroelectric activity of FF microtubes (Fig. 5C). The pyroelectric coefficient was found to be ~2 μC m^{-2} K^{-1}, comparable to that of conventional inorganic semiconductive pyroelectrics such as AlN or ZnO (79).

The surface charges generated in response to an external stress of the assemblies can yield piezoelectricity (78). Analysis of the in-plane (d_{15}) shear piezoelectric effect of FF nanotubes has shown the effective d_{15} coefficient of a tube ≥200 nm in diameter to be comparable to that of $LiNbO_3$, the classical inorganic transducer (80). The lateral signal calibration yields sufficiently high effective piezoelectric coefficient values of at least 60 pm V^{-1}; by contrast, the piezoelectric coefficient of sclera collagen, 20 pm V^{-1}, is the highest known for a biomaterial (80). In addition, the FF nanotubes demonstrate linear deformation without irreversible degradation in a broad range of driving voltages up to 16 V, potentially facilitating their use as nanoscale piezoelectrics in various biotechnological and medicinal applications.

In the presence of an external electric field, the vertical FF microrod arrays can be organized on a substrate (81). The arrays offer improved piezo-electric properties, showing uniform polarization in two opposite directions, with the effective pi-ezoelectric constant d_{33} reaching 17.9 pm V^{-1}. Therefore, these microrod arrays can be used to fabricate a power generator (Fig. 5D) whose power density substantially exceeds that of similar devices (Fig. 5E), with open-circuit voltage of 1.4 V and power density of 3.3 nW cm^{-2} (Fig. 5F) (81).

The induced polarization illustrates that peptide self-assemblies can be directionally aligned on electrodes by an external electric field, such as that used in dielectrophoresis. In particular, the efficiency of binding of the nanostructures to the substrates can be measured by the impedance increase between the electrodes, resulting from changes in the electric field lines and current distribution (82). This can allow the fabrication of sensitive and versatile sensors based on peptide self-assemblies (83). For example, self-assembling nanotubes formed by the bola-amphiphilic peptide bis(*N*-α-amidoglycylglycine)-1,7-heptane dicarboxylate were trapped in the gap between adjacent electrodes by positive dielectrophoresis (84). After conjugating sheep polyclonal antibody to herpes simplex virus–2 (HSV-2), a high-sensitivity, label-free pathogen detection sensor chip was fabricated. This chip can detect HSV-2 at a concentration of $<10^2$ pfu ml^{-1} within 1 hour (84). Furthermore, this bioinspired chip is able to quantitatively target multiple pathogens by conjugating the corresponding antibodies, hence offering multiplexed detection capabilities and cost-effective reusability along with outstanding sensitivity (85). When integrating a peptide with a high affinity to lead ions (Pb^{2+}), the nanotubular sensor configuration can efficiently detect, immobilize, concentrate, and metallize ultralow levels of Pb^{2+} (86).

Ultrasensitive peptide-based devices

Because electron transfer between spatially aligned aromatic systems can promote electric conductivity, FF nanotubes can increase the sensitivity of coated electrochemical electrodes (87). The biomodified electrochemical sensory platform can therefore exhibit nonmediated electron transfer, short detection time, large current density, high stability, and reproducibility for antigen detection (88). Such a biosensor enabled a sensitive determination of glucose (detected substrate) by monitoring the hydrogen peroxide produced via hydrolysis of glucose by the conjugated glucose oxidase (GOx, antenna) (Fig. 6A). Moreover, when integrated with ethanol dehydrogenase (antenna), the marked electrocatalytic activity toward NADH (reduced nicotinamide adenine dinucleotide) enabled sensitive detection of ethanol (detected substrate) (88). Similarly, the extended functional surface area facilitated the use of an electrode modified with FF tubular nanoarrays as an ultrasensitive biosensor, with phenol detection sensitivity exceeding that of a native electrode by a factor of 17 and higher sensitivity relative to electrodes modified with carbon nanotubes (89).

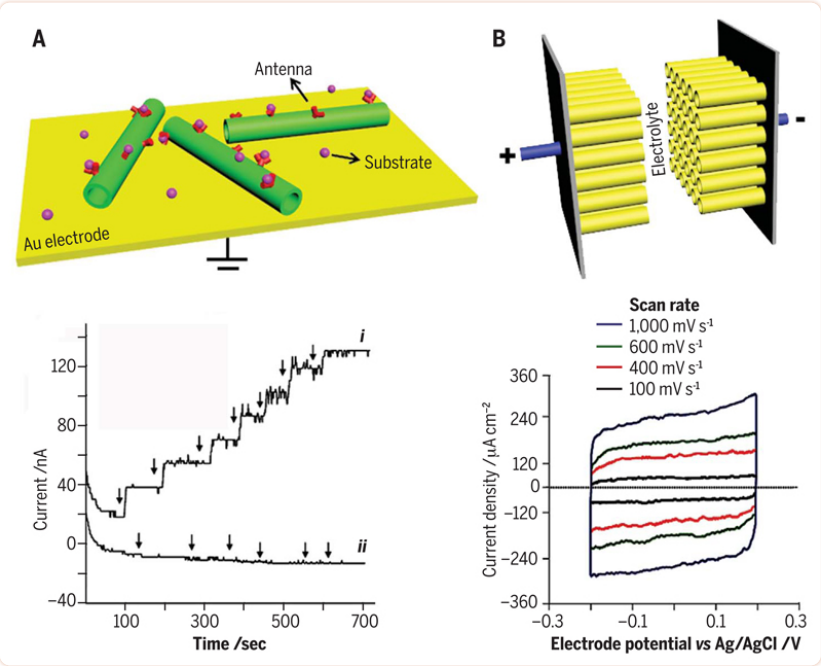

Fig. 6

Electrochemical performance of FF self-assembling semiconductors.

(A) Top: Schematic mechanism of FF nanotube-based biosensors. The antennas conjugated on FF nanotubes recognize and capture the detected substrates, and the electrical signals resulting from the electrochemical reactions can be transmitted by the nanotubes and recorded. Bottom: Amperometric response to successive additions of β-D-glucose on (i) a GOx-conjugated FF nanotube-coated electrode and (ii) a bare electrode. Arrows indicate the successive increases of glucose concentration. [Adapted from (88)] **(B)** Top: Cartoon model of FF tubular nanoarray–based ultracapacitors. The orderly, multiporous nanotube arrays can increase the effective activation area of the modified electrode and enhance the electric conductivity. Bottom: Cyclic voltammograms of FF nanoarray–coated carbon electrodes at different scan rates, showing typical rectangular double-layer capacitance behavior. [Adapted from (37)]

Energy-storage properties

The FF vertical nanoarrays can also increase the effective activation area of the modified electrodes and enhance the electric conductivity (37, 90), showing a cyclic voltammogram curve of a typical double-layer capacitance (Fig. 6B, top) (37). Thus, the charge-discharge process of the modified electrodes is purely electrostatic and the current is independent of the applied potential (Fig. 6B, bottom). The critical factor allowing the electrolyte ions to easily accumulate on the modified electrode surface is a wetting process by aqueous electrolytes in the nanoscale hydrophilic channels inside the nanotubes (Fig. 3A) (90). These findings demonstrate the potential of FF nanoarrays as high-capacity ultracapacitors for fast charging in energy storage applications, such as batteries for mobile devices and electric vehicles.

Future perspectives

Extensive studies have revealed that semiconductive features are inherent properties of some peptide-based nanostructures, exhibiting notable physicochemical characteristics that can allow the development of bioinspired entities into functional materials. Because they are eco-friendly, morphologically and functionally flexible, and easy to prepare, modify, and modulate, these supramolecular nanomaterials can serve as promising alternatives to the widely used inorganic counterparts. The ability to conjugate external functional moieties links the supramolecular materials with conventional organic semiconductors, producing hybrid or extrinsic semiconductors with enhanced performance. As a result of their bioinspired nature, short peptide self-assemblies can be used in biotechnological and medical fields, thus bridging the semiconductor and biological worlds. Yet this field is remarkably interdisciplinary and is still in its infancy. For peptide self-assemblies to become reliable and widely used semiconductors, several challenges still need to be met, including understanding the relationships between nanostructural morphologies and functions, identifying the molecular mechanisms underlying the physicochemical properties, control and doping of the semiconductivity, and conversion from scientific progress to industrial engineering.

Studies on short peptide self-assemblies can also shed light on the roles of protein semiconductivity in physiology and pathology, thereby promoting research into the connection between the semiconductive properties of misfolded proteins and degenerative symptoms. Such research would offer opportunities to visually track the assembly process and investigate the mechanisms controlling neurodegeneration diseases, possibly leading to the development of optimal therapeutic solutions.

In the long term, self-assembling short peptide semiconductors can be used to develop autonomous biomachines that operate within biological systems in vivo. This may allow, for example, direct, label-free, real-time monitoring and sensing of a wide variety of metabolic activities, as well as analysis of (and possibly interference with) biological systems. It may be possible to alleviate motor disorders, such as epilepsy and Parkinson's disease, by using such semiconductive systems to interfere with neuronal electrical impulses. Such future technologies will have enormous scientific, social, and economic implications.

Background

The increasing demand for environmentally friendly organic semiconductors that can be easily fabricated and tuned has inspired scientists to design self-assembling peptide nanostructures with enhanced semiconducting characteristics. Recently designed bioinspired peptide semiconductors display various supramolecular morphologies with diverse optical and electrical properties, including intrinsic fluorescence, which facilitates real-time detection and quantitative assessment of the self-association process without a need for external conjugation. These assemblies have also been studied for their potential use in ferroelectric-related devices and ultrasensitive electrochemical sensors. In addition to their low-cost fabrication and structural diversity, bioinspired self-assembling peptide semiconductors may serve as candidates for advanced interdisciplinary functional nanostructures. Promotion of the design principles of peptide-based supramolecular materials is thus of great interest for both scientific and engineering development.

Advances

Short peptides, specifically those containing aromatic amino acids, can self-assemble into a wide variety of supramolecular structures that are kinetically or thermodynamically stable; the representative models are diphenylalanine and phenylalanine-tryptophan. Different assembly strategies can be used to generate specific functional organizations and nanostructural arrays, resulting in finely tunable morphologies with controllable semiconducting characteristics. Such strategies include molecular modification, microfluidics, co-assembly, physical or chemical vapor deposition, and introduction of an external electromagnetic field. Density functional theory simulations have revealed that extensive, directional aromatic interactions and hydrogen-bonding networks lead to the formation of quantum confined domains within the nanostructures, underlying the molecular origin of their intrinsic semiconductivity. These computational studies provide a conceptual framework for the tunability of the semiconductivity of a peptide assembly, and also demonstrate the feasibility of theoretical probing of the mechanisms leading to band gap formation and the subsequent design of building blocks with desired electronic properties. Recent studies have further elucidated some remarkable physicochemical features of the bioinspired supramolecular semiconductors, including absorption spectra characteristic of one-dimensional quantum dots or two-dimensional quantum wells, photoluminescence emission in the visible spectrum, optical waveguiding, temperature-dependent electrical conductivity, ferroelectric (piezoelectric, pyroelectric) properties, and electrochemical properties useful in ultrasensitive detectors and ultracapacitors.

Outlook

Semiconductive materials are at the foundation of the modern electronics and optics industries. Self-assembling peptide nanomaterials may serve as an alternative source for the semiconductor industry because they are eco-friendly, morphologically and functionally flexible, and easy to prepare, modify, and dope. Moreover, the diverse bottom-up methodologies of peptide self-assembly facilitate easy and cost-effective device fabrication, with the ability to integrate external functional moieties. For example, the coassembly of peptides and electron donors or acceptors can be used to construct n-p junctions, and vapor deposition technology can be applied to manufacture custom-designed electronics and chips on various substrates.

The inherent bioinspired nature of self-assembling peptide nanostructures allows them to bridge the gap between the semiconductor world and biological systems, thus making them useful for applications in fundamental biology and health care research. Short peptide self-assemblies may shed light on the roles of protein semiconductivity in physiology and pathology. For example, research into the relationship between the semiconductive properties of misfolded polypeptides characteristic of various neurodegenerative diseases and the resulting symptoms may offer opportunities to investigate the mechanisms controlling such ailments and to develop therapeutic solutions. Finally, self-assembling short peptide semiconductors could be used to develop autonomous biomachines operating within biological systems. This would allow, for example, direct, label-free, real-time monitoring of a variety of metabolic activities, and even interference with biological systems.

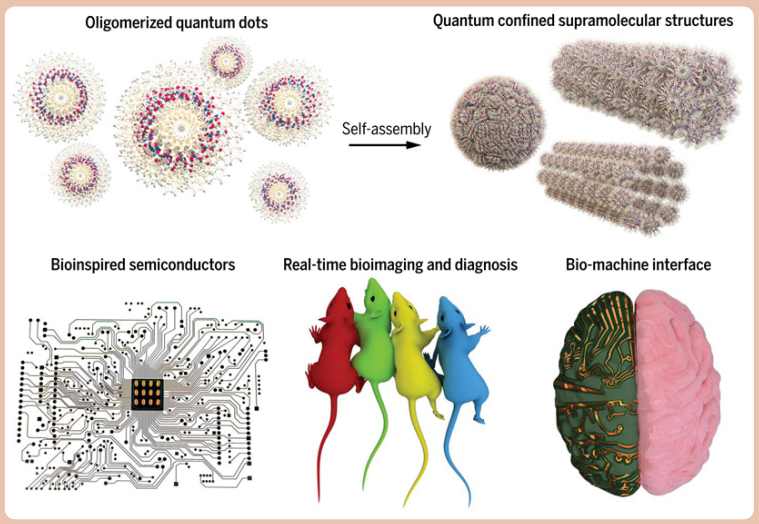

Peptide building blocks self-assemble into quantum confined supramolecular semiconductors.

These bioinspired functional materials can serve as organic semiconductors. Their ability to connect the semiconductor field and the biological world will facilitate the incorporation of semiconductivity into fundamental biomedical and health care applications.

Peptide-based semiconductors

For semiconductors, one often thinks of inorganic materials, such as doped silicon, or aromatic organic polymers and small molecules. Tao et al. review progress in making semiconductors based on self-assembling short peptides. The structures that form show extensive π and hydrogen bonding leading to a range of semiconductor properties, which can be tuned through doping or functionalization of the peptide sequences. These materials may shed light on biological semiconductors or provide an alternative for constructing biocompatible and therapeutic materials.

Science, this issue p. aam9756

Acknowledgments

Supported by grants from the Israeli National Nanotechnology Initiative, the Helmsley Charitable Trust for a Focal Technology Area on Nanomedicine for Personalized Theranostics, and the European Research Council under the European Union's Horizon 2020 research and innovation program (no. 694426) (E.G.). We thank S. Rencus-Lazar for language editing and members of the Gazit laboratory for helpful discussions.

References

1. Wu Y, et al. Inorganic semiconductor nanowires: Rational growth, assembly, and novel properties. *Chem Eur J.* 2002;8:1260–1268. doi: 10.1002/1521-3765(20020315)8:6<1260::AID-CHEM1260>3.0.CO;2-Q. [PubMed] [CrossRef] [Google Scholar]

2. Fang XS, Bando Y, Gautam UK, Ye C, Golberg D. Inorganic semiconductor nanostructures and their field-emission applications. *J Mater Chem.* 2008;18:509–522. doi: 10.1039/B712874F. [CrossRef] [Google Scholar]

3. Takimiya K, Osaka I, Mori T, Nakano M. Organic semiconductors based on [1]benzothieno[3,2-*b*][1] benzothiophene substructure. *Acc Chem Res.* 2014;47:1493–1502. doi: 10.1021/ar400282g. [PubMed] [CrossRef] [Google Scholar]

4. Marks TJ. Electrically conductive metallomacrocyclic assemblies. *Science.* 1985;227:881–889. doi: 10.1126/science.227.4689.881. [PubMed] [CrossRef] [Google Scholar]

5. Turek P, et al. A new series of molecular semiconductors: Phthalocyanine radicals. *J Am Chem Soc.* 1987;109:5119–5122. doi: 10.1021/ja00251a012. [CrossRef] [Google Scholar]

6. Van Nostrum CF, Nolte RJM. Functional supramolecular materials: Self-assembly of phthalocyanines and porphyrazines. *Chem Commun.* 1996;1996:2385–2392. doi: 10.1039/cc9960002385. [CrossRef] [Google Scholar]

7. Aida T, Meijer EW, Stupp SI. Functional supramolecular polymers. *Science.* 2012;335:813–817. doi: 10.1126/science.1205962. [PMC free article] [PubMed] [CrossRef] [Google Scholar]

8. Hauser CAE, Zhang S. Nanotechnology: Peptides as biological semiconductors. *Nature.* 2010;468:516–517. doi: 10.1038/468516a. [PubMed] [CrossRef] [Google Scholar]

9. Gazit E. Peptide nanostructures: Aromatic dipeptides light up. *Nat Nanotechnol.* 2016;11:309–310. doi: 10.1038/nnano.2015.321. [PubMed] [CrossRef] [Google Scholar]

10. Weingarten AS, et al. Self-assembling hydrogel scaffolds for photocatalytic hydrogen production. *Nat Chem.* 2014;6:964–970. doi: 10.1038/nchem.2075. [PMC free article] [PubMed] [CrossRef] [Google Scholar]

11. Bai S, et al. Differential self-assembly and tunable emission of aromatic peptide *bola*-amphiphiles containing perylene bisimide in polar solvents including water. *Langmuir.* 2014;30:7576–7584. doi: 10.1021/la501335e. [PubMed] [CrossRef] [Google Scholar]

12. Eakins GL, et al. Functional organic semiconductors assembled via natural aggregating peptides. *Adv Funct Mater.* 2015;25:5640–5649. doi: 10.1002/adfm.201502255. [CrossRef] [Google Scholar]

13. Eakins GL, et al. Thermodynamic factors impacting the peptide-driven self-assembly of perylene diimide nanofibers. *J Phys Chem B.* 2014;118:8642–8651. doi: 10.1021/jp504564s. [PubMed] [CrossRef] [Google Scholar]

14. Draper ER, et al. pH-directed aggregation to control photoconductivity in self-assembled perylene bisimides. *Chem.* 2017;2:716–731. doi: 10.1016/j.chempr.2017.03.022. [CrossRef] [Google Scholar]

15. Chan FT, Pinotsi D, Schierle GSK, Kaminski CF. Structure-specific intrinsic fluorescence of protein amyloids used to study their kinetics of aggregation. In: Uversky V, Lyubchenko Y, editors. *Bio-Nanoimaging: Protein Misfolding and Aggregation.* Elsevier; 2014. pp. 147–155. [Google Scholar]

16. Pinotsi D, Buell AK, Dobson CM, Kaminski Schierle GS, Kaminski CF. A label-free, quantitative assay of amyloid fibril growth based on intrinsic fluorescence. *ChemBioChem.* 2013;14:846–850. doi: 10.1002/cbic.201300103. [PMC free article] [PubMed] [CrossRef] [Google Scholar]

17. Kaminski Schierle GS, et al. A FRET sensor for non-invasive imaging of amyloid formation in vivo. *ChemPhysChem.* 2011;12:673–680. doi: 10.1002/cphc.201000996. [PMC free article] [PubMed] [CrossRef] [Google Scholar]

18. Santhanamoorthi N, et al. Diphenylalanine peptide nanotube: Charge transport, band gap and its relevance to potential biomedical applications. *Adv Mat Lett.* 2011;2:100–105. doi: 10.5185/amlett.2010.12223. [CrossRef] [Google Scholar]

19. Adler-Abramovich L, et al. Self-assembled organic nanostructures with metallic-like stiffness. *Angew Chem Int Ed.* 2010;49:9939–9942. doi: 10.1002/anie.201002037. [PubMed] [CrossRef] [Google Scholar]

20. Kol N, et al. Self-assembled peptide nanotubes are uniquely rigid bioinspired supramolecular structures. *Nano Lett.* 2005;5:1343–1346. doi: 10.1021/nl0505896. [PubMed] [CrossRef] [Google Scholar]

21. Truong WT, Su Y, Gloria D, Braet F, Thordarson P. Dissolution and degradation of Fmoc-diphenylalanine self-assembled gels results in necrosis at high concentrations *in vitro*. *Biomater Sci.* 2015;3:298–307. doi: 10.1039/C4BM00244J. [PubMed] [CrossRef] [Google Scholar]

22. Reches M, Gazit E. Casting metal nanowires within discrete self-assembled peptide nanotubes. *Science.* 2003;300:625–627. doi: 10.1126/science.1082387. [PubMed] [CrossRef] [Google Scholar]

23. Tan YN, Lee JY, Wang DIC. Uncovering the design rules for peptide synthesis of metal nanoparticles. *J Am Chem Soc.* 2010;132:5677–5686. doi: 10.1021/ja907454f. [PubMed] [CrossRef] [Google Scholar]

24. Zhang S. Fabrication of novel biomaterials through molecular self-assembly. *Nat Biotechnol.* 2003;21:1171–1178. doi: 10.1038/nbt874. [PubMed] [CrossRef] [Google Scholar]

25. Tao K, Levin A, Adler-Abramovich L, Gazit E. Fmoc-modified amino acids and short peptides: Simple bio-inspired building blocks for the fabrication of functional materials. *Chem Soc Rev.* 2016;45:3935–3953. doi: 10.1039/C5CS00889A. [PubMed] [CrossRef] [Google Scholar]

26. Kresse G, Hafner J. *Ab initio* molecular-dynamics simulation of the liquid-metal-amorphous-semiconductor transition in germanium. *Phys Rev B.* 1994;49:14251–14269. doi: 10.1103/PhysRevB.49.14251. [PubMed] [CrossRef] [Google Scholar]

27. Adler-Abramovich L, Gazit E. The physical properties of supramolecular peptide assemblies: From building block association to technological applications. *Chem Soc Rev.* 2014;43:6881–6893. doi: 10.1039/C4CS00164H. [PubMed] [CrossRef] [Google Scholar]

28. Kim S, Kim JH, Lee JS, Park CB. Beta-sheet-forming, self-assembled peptide nanomaterials towards optical, energy, and healthcare applications. *Small.* 2015;11:3623–3640. doi: 10.1002/smll.201500169. [PubMed] [CrossRef] [Google Scholar]

29. Yan X, Zhu P, Li J. Self-assembly and application of diphenylalanine-based nanostructures. *Chem Soc Rev.* 2010;39:1877–1890. doi: 10.1039/b915765b. [PubMed] [CrossRef] [Google Scholar]

30. Zhu P, Yan X, Su Y, Yang Y, Li J. Solvent-induced structural transition of self-assembled dipeptide: From organogels to microcrystals. *Chem Eur J.* 2010;16:3176–3183. doi: 10.1002/chem.200902139. [PubMed] [CrossRef] [Google Scholar]

31. Mason TO, et al. Expanding the solvent chemical space for self-assembly of dipeptide nanostructures. *ACS Nano.* 2014;8:1243–1253. doi: 10.1021/nn404237f. [PubMed] [CrossRef] [Google Scholar]

32. Liu X, et al. Transformation of dipeptide-based organogels into chiral crystals by cryogenic treatment. *Angew Chem.* 2017;129:2704–2707. doi: 10.1002/ange.201612024. [PubMed] [CrossRef] [Google Scholar]

33. Reches M, Gazit E. Controlled patterning of aligned self-assembled peptide nanotubes. *Nat Nanotechnol.* 2006;1:195–200. doi: 10.1038/nnano.2006.139. [PubMed] [CrossRef] [Google Scholar]

34. Hill RJA, et al. Alignment of aromatic peptide tubes in strong magnetic fields. *Adv Mater.* 2007;19:4474–4479. doi: 10.1002/adma.200700590. [CrossRef] [Google Scholar]

35. Chen J, Qin S, Wu X, Chu AP. Morphology and pattern control of diphenylalanine self-assembly via evaporative dewetting. *ACS Nano.* 2016;10:832–838. doi: 10.1021/acsnano.5b05936. [PubMed] [CrossRef] [Google Scholar]

36. Hendler N, et al. Formation of well-organized self-assembled films from peptide nanotubes. *Adv Mater.* 2007;19:1485–1488. doi: 10.1002/adma.200602265. [CrossRef] [Google Scholar]

37. Adler-Abramovich L, et al. Self-assembled arrays of peptide nanotubes by vapour deposition. *Nat Nanotechnol.* 2009;4:849–854. doi: 10.1038/nnano.2009.298. [PubMed] [CrossRef] [Google Scholar]

38. Vasudev MC, et al. Vertically aligned peptide nanostructures using plasma-enhanced chemical vapor deposition. *Biomacromolecules.* 2014;15:533–540. doi: 10.1021/bm401491k. [PubMed] [CrossRef] [Google Scholar]

39. Ryu J, Park CB. High-temperature self-assembly of peptides into vertically well-aligned nanowires by aniline vapor. *Adv Mater.* 2008;20:3754–3758. doi: 10.1002/adma.200800364. [CrossRef] [Google Scholar]

40. Ryu J, Park CB. Synthesis of diphenylalanine/polyaniline core/shell conducting nanowires by peptide self-assembly. *Angew Chem Int Ed.* 2009;48:4820–4823. doi: 10.1002/anie.200900668. [PubMed] [CrossRef] [Google Scholar]

41. Yan X, Li J, Möhwald H. Self-assembly of hexagonal peptide microtubes and their optical waveguiding. *Adv Mater.* 2011;23:2796–2801. doi: 10.1002/adma.201100353. [PubMed] [CrossRef] [Google Scholar]

42. Arnon ZA, et al. Dynamic microfluidic control of supramolecular peptide self-assembly. *Nat Commun.* 2016;7:13190. doi: 10.1038/ncomms13190. [PMC free article] [PubMed] [CrossRef] [Google Scholar]

43. Guo C, et al. Expanding the nanoarchitectural diversity through aromatic di- and tri-peptide coassembly: Nanostructures and molecular mechanisms. *ACS Nano.* 2016;10:8316–8324. doi: 10.1021/acsnano.6b02739. [PubMed] [CrossRef] [Google Scholar]

44. Adler-Abramovich L, et al. Controlling the physical dimensions of peptide nanotubes by supramolecular polymer coassembly. *ACS Nano.* 2016;10:7436–7442. doi: 10.1021/acsnano.6b01587. [PubMed] [CrossRef] [Google Scholar]

45. Mahler A, Reches M, Rechter M, Cohen S, Gazit E. Rigid, self-assembled hydrogel composed of a modified aromatic dipeptide. *Adv Mater.* 2006;18:1365–1370. doi: 10.1002/adma.200501765. [CrossRef] [Google Scholar]

46. Smith AM, et al. Fmoc-diphenylalanine self assembles to a hydrogel via a novel architecture based on π-π interlocked β-sheets. *Adv Mater.* 2008;20:37–41. doi: 10.1002/adma.200701221. [CrossRef] [Google Scholar]

47. Levin A, et al. Ostwald's rule of stages governs structural transitions and morphology of dipeptide supramolecular polymers. *Nat Commun.* 2014;5:5219. doi: 10.1038/ncomms6219. [PubMed] [CrossRef] [Google Scholar]

48. Amdursky N, Molotskii M, Gazit E, Rosenman G. Self-assembled bioinspired quantum dots: Optical properties. *Appl Phys Lett.* 2009;94:261907. doi: 10.1063/1.3167354. [CrossRef] [Google Scholar]

49. Nalluri SKM, et al. Conducting nanofibers and organogels derived from the self-assembly of tetrathiafulvalene-appended dipeptides. *Langmuir.* 2014;30:12429–12437. doi: 10.1021/la503459y. [PubMed] [CrossRef] [Google Scholar]

50. Yan X, et al. Reversible transitions between peptide nanotubes and vesicle-like structures including theoretical modeling studies. *Chem Eur J.* 2008;14:5974–5980. doi: 10.1002/chem.200800012. [PubMed] [CrossRef] [Google Scholar]

51. Charalambidis G, et al. A switchable self-assembling and disassembling chiral system based on a porphyrin-substituted phenylalanine-phenylalanine motif. *Nat Commun.* 2016;7:12657. doi: 10.1038/ncomms12657. [PMC free article] [PubMed] [CrossRef] [Google Scholar]

52. Nielsen PE, Egholm M, Berg RH, Buchardt O. Sequence-selective recognition of DNA by strand displacement with a thymine-substituted polyamide. *Science.* 1991;254:1497–1500. doi: 10.1126/science.1962210. [PubMed] [CrossRef] [Google Scholar]

53. Berger O, et al. Light-emitting self-assembled peptide nucleic acids exhibit both stacking interactions and Watson-Crick base pairing. *Nat Nanotechnol.* 2015;10:353–360. doi: 10.1038/nnano.2015.27. [PubMed] [CrossRef] [Google Scholar]

54. Amdursky N, Molotskii M, Gazit E, Rosenman G. Elementary building blocks of self-assembled peptide nanotubes. *J Am Chem Soc.* 2010;132:15632–15636. doi: 10.1021/ja104373e. [PubMed] [CrossRef] [Google Scholar]

55. Guo C, Luo Y, Zhou R, Wei G. Probing the self-assembly mechanism of diphenylalanine-based peptide nanovesicles and nanotubes. *ACS Nano.* 2012;6:3907–3918. doi: 10.1021/nn300015g. [PubMed] [CrossRef] [Google Scholar]

56. Görbitz CH. The structure of nanotubes formed by diphenylalanine, the core recognition motif of Alzheimer's β-amyloid polypeptide. *Chem Commun.* 2006;2006:2332–2334. doi: 10.1039/B603080G. [PubMed] [CrossRef] [Google Scholar]

57. Azuri I, Adler-Abramovich L, Gazit E, Hod O, Kronik L. Why are diphenylalanine-based peptide nanostructures so rigid? Insights from first principles calculations. *J Am Chem Soc.* 2014;136:963–969. doi: 10.1021/ja408713x. [PubMed] [CrossRef] [Google Scholar]

58. Chan FTS, et al. Protein amyloids develop an intrinsic fluorescence signature during aggregation. *Analyst.* 2013;138:2156–2162. doi: 10.1039/c3an36798c. [PMC free article] [PubMed] [CrossRef] [Google Scholar]

59. Pinotsi D, et al. Proton transfer and structure-specific fluorescence in hydrogen bond-rich protein structures. *J Am Chem Soc.* 2016;138:3046–3057. doi: 10.1021/jacs.5b11012. [PubMed] [CrossRef] [Google Scholar]

60. Amdursky N. Enhanced solid-state electron transport via tryptophan containing peptide networks. *Phys Chem Chem Phys.* 2013;15:13479–13482. doi: 10.1039/c3cp51748a. [PubMed] [CrossRef] [Google Scholar]

61. Akdim B, Pachter R, Naik RR. Self-assembled peptide nanotubes as electronic materials: An evaluation from first-principles calculations. *Appl Phys Lett.* 2015;106:183707. doi: 10.1063/1.4921012. [CrossRef] [Google Scholar]

62. Wang M, Xiong S, Wu X, Chu PK. Effects of water molecules on photoluminescence from hierarchical peptide nanotubes and water probing capability. *Small.* 2011;7:2801–2807. doi: 10.1002/smll.201100353. [PubMed] [CrossRef] [Google Scholar]

63. Rosenman G, et al. Bioinspired peptide nanotubes: Deposition technology, basic physics and nanotechnology applications. *J Pept Sci.* 2011;17:75–87. doi: 10.1002/psc.1326. [PubMed] [CrossRef] [Google Scholar]

64. Amdursky N, Gazit E, Rosenman G. Quantum confinement in self-assembled bioinspired peptide hydrogels. *Adv Mater.* 2010;22:2311–2315. doi: 10.1002/adma.200904034. [PubMed] [CrossRef] [Google Scholar]

65. Nikitin T, Kopyl S, Shur VY, Kopelevich YV, Kholkin AL. Low-temperature photoluminescence in self-assembled diphenylalanine microtubes. *Phys Lett A.* 2016;380:1658–1662. doi: 10.1016/j.physleta.2016.02.043. [CrossRef] [Google Scholar]

66. Amdursky N, et al. Blue luminescence based on quantum confinement at peptide nanotubes. *Nano Lett.* 2009;9:3111–3115. doi: 10.1021/nl9008265. [PubMed] [CrossRef] [Google Scholar]

67. Amdursky N, Koren I, Gazit E, Rosenman G. Adjustable photoluminescence of peptide nanotubes coatings. *J Nanosci Nanotechnol.* 2011;11:9282–9286. doi: 10.1166/jnn.2011.4278. [PubMed] [CrossRef] [Google Scholar]

68. Erwin SC, et al. Doping semiconductor nanocrystals. *Nature.* 2005;436:91–94. doi: 10.1038/nature03832. [PubMed] [CrossRef] [Google Scholar]

69. Tsukazaki A, et al. Repeated temperature modulation epitaxy for p-type doping and light-emitting diode based on ZnO. *Nat Mater.* 2005;4:42–46. doi: 10.1038/nmat1284. [CrossRef] [Google Scholar]

70. Fan Z, Sun L, Huang Y, Wang Y, Zhang M. Bioinspired fluorescent dipeptide nanoparticles for targeted cancer cell imaging and real-time monitoring of drug release. *Nat Nanotechnol.* 2016;11:388–394. doi: 10.1038/nnano.2015.312. [PubMed] [CrossRef] [Google Scholar]

71. Yan X, Su Y, Li J, Früh J, Möhwald H. Uniaxially oriented peptide crystals for active optical waveguiding. *Angew Chem Int Ed.* 2011;50:11186–11191. doi: 10.1002/anie.201103941. [PubMed] [CrossRef] [Google Scholar]

72. Yu PY, Cardona M. *Fundamentals of Semiconductors.* Springer; 2010. pp. 203–241. [Google Scholar]

73. Lee JS, et al. Self-assembly of semiconducting photoluminescent peptide nanowires in the vapor phase. *Angew Chem Int Ed.* 2011;50:1164–1167. doi: 10.1002/anie.201003446. [PubMed] [CrossRef] [Google Scholar]

74. Amit M, Cheng G, Hamley IW, Ashkenasy N. Conductance of amyloid β based peptide filaments: Structure-function relations. *Soft Matter.* 2012;8:8690–8696. doi: 10.1039/c2sm26017d. [CrossRef] [Google Scholar]

75. Amit M, et al. Hybrid proton and electron transport in peptide fibrils. *Adv Funct Mater.* 2014;24:5873–5880. doi: 10.1002/adfm.201401111. [CrossRef] [Google Scholar]

76. Heredia A, et al. Temperature-driven phase transformation in self-assembled diphenylalanine peptide nanotubes. *J Phys D.* 2010;43:462001. doi: 10.1088/0022-3727/43/46/462001. [CrossRef] [Google Scholar]

77. Gan Z, Wu X, Zhu X, Shen J. Light-induced ferroelectricity in bioinspired self-assembled diphenylalanine nanotubes/microtubes. *Angew Chem Int Ed.* 2013;52:2055–2059. [PubMed] [Google Scholar]

78. Xu Y. *Ferroelectric Materials and Their Applications.* North-Holland Elsevier Science; 1991. [Google Scholar]

79. Esin A, et al. Pyroelectric effect and polarization instability in self-assembled diphenylalanine microtubes. *Appl Phys Lett.* 2016;109:142902. doi: 10.1063/1.4962652. [CrossRef] [Google Scholar]

80. Kholkin A, Amdursky N, Bdikin I, Gazit E, Rosenman G. Strong piezoelectricity in bioinspired peptide nanotubes. *ACS Nano.* 2010;4:610–614. doi: 10.1021/nn901327v. [PubMed] [CrossRef] [Google Scholar]

81. Nguyen V, Zhu R, Jenkins K, Yang R. Self-assembly of diphenylalanine peptide with controlled polarization for power generation. *Nat Commun.* 2016;7:13566. doi: 10.1038/ncomms13566. [PMC free article] [PubMed] [CrossRef] [Google Scholar]

82. de la Rica R, Matsui H. Applications of peptide and protein-based materials in bionanotechnology. *Chem Soc Rev.* 2010;39:3499–3509. doi: 10.1039/b917574c. [PMC free article] [PubMed] [CrossRef] [Google Scholar]

83. Gao X, Matsui H. Peptide-based nanotubes and their applications in bionanotechnology. *Adv Mater.* 2005;17:2037–2050. doi: 10.1002/adma.200401849. [CrossRef] [Google Scholar]

84. de la Rica R, Mendoza E, Lechuga LM, Matsui H. Label-free pathogen detection with sensor chips assembled from Peptide nanotubes. *Angew Chem Int Ed.* 2008;47:9752–9755. doi: 10.1002/anie.200804299. [PMC free article] [PubMed] [CrossRef] [Google Scholar]

85. de la Rica R, Pejoux C, Fernandez-Sanchez C, Baldi A, Matsui H. Peptide-nanotube biochips for label-free detection of multiple pathogens. *Small.* 2010;6:1092–1095. doi: 10.1002/smll.201000151. [PMC free article] [PubMed] [CrossRef] [Google Scholar]

86. de la Rica R, Mendoza E, Matsui H. Bioinspired target-specific crystallization on peptide nanotubes for ultrasensitive Pb ion detection. *Small.* 2010;6:1753–1756. doi: 10.1002/smll.201000489. [PMC free article] [PubMed] [CrossRef] [Google Scholar]

87. Yemini M, Reches M, Rishpon J, Gazit E. Novel electrochemical biosensing platform using self-assembled peptide nanotubes. *Nano Lett.* 2005;5:183–186. doi: 10.1021/nl0484189. [PubMed] [CrossRef] [Google Scholar]

88. Yemini M, Reches M, Gazit E, Rishpon J. Peptide nanotube-modified electrodes for enzyme-biosensor applications. *Anal Chem.* 2005;77:5155–5159. doi: 10.1021/ac050414g. [PubMed] [CrossRef] [Google Scholar]

89. Adler-Abramovich L, Badihi-Mossberg M, Gazit E, Rishpon J. Characterization of peptide-nanostructure-modified electrodes and their application for ultrasensitive environmental monitoring. *Small.* 2010;6:825–831. doi: 10.1002/smll.200902186. [PubMed] [CrossRef] [Google Scholar]

90. Beker P, Koren I, Amdursky N, Gazit E, Rosenman G. Bioinspired peptide nanotubes as supercapacitor electrodes. *J Mater Sci.* 2010;45:6374–6378. doi: 10.1007/s10853-010-4624-z. [CrossRef] [Google Scholar]